THE 7th INTERNATIONAL CONFERENCE ON SHOT PEENING ICSP 7 INSTITUTE OF PRECISION MECHANICS WARSAW, POLAND

NUMERICAL SIMULATION OF MULTIPLE SHOT IMPACT

S.T.S. Al-Hassani
Department of Mechanical Engineering, The University of Manchester Institute of Science and Technology, P.O. Box 88, Manchester M60 1QD, U.K.
K. Kormi, K. and D.C. Webb
School of Engineering, Leeds Metropolitan University, Calverley Street, Leeds LS1 3HE, UK.

ABSTRACT

This paper reports the results obtained from a numerical simulation using the Finite Element Method of three cases of shot peening:
1) single shot impacts normal to the target with three different impact velocities;
2) a five shot successive series of normal impacts along a line and overlap, causing ovalisation of the indentation;
3) a single shot impact at an oblique angle to the peened surface.
In the analyses the material was considered to exhibit linear-elastic behaviour with a non-linear work hardening characteristic, and a strain rate dependency. The shakedown effect is a natural consequence of the material elastic plastic model behaviour used in this solution procedure. Several other important features associated with material strain-rate dependency and work hardening, hitherto unreported in the literature, are observed and discussed in detail. Possible explanations of the results are presented.

KEY WORDS

Finite Element Method, residual stress, normal impact, multiple impact

INTRODUCTION

Central to the problem of shot peening is the multiple impact of hard spheres on a surface producing a hardened layer with a compressive residual stress whose intensity and distribution slows down fatigue and crack initiation and growth.

Study of the contact problem between elastic and elastic-plastic materials resulting from the loading of two bodies was pioneered by Hertz [1]. Other important work on the response of a semi-infinite space to concentrated point loading was carried out by Boussinique [2]. A comprehensive source of reference material can be found in the classic works of Timoshenko and Goodier [3] and Sneddon [4]. Further sources of references on indentation and allied subjects are given by Goldsmith [5] and Johnson [6]. Aspects of indentation, such as the effects of physical properties of spherical indentors on hardness, and the correlation between the hardness and stress flow, have been reported in [7,8]. The application of a non-linear FEM was employed to further the understanding of the mechanism of the shot peening process in [9,10,11].

Several models based on elastic-perfectly plastic constitutive material behaviour are summarised in [12,13-16]. What emerges is that shot peening is an effective procedure for increasing the fatigue life of machine parts and helps to guard against the spread of a tensile stress field that may occur due to the presence of imperfections not visible at the exposed surfaces. However, there is very little analytical work that takes into consideration material non-linear work hardening, strain rate effects, or multiple out-of-line collisions. These issues are addressed in this paper by using the FEM. The relationship between material hardness and residual stresses is reported in [17] and the effects of the material behaviour from a theoretical point of view are reported in [18]. Experimental work on the dynamics of indentation and the influence of the strain-rate on the plastic flow behaviour of a ductile material is examined in [19], while the effects of shot peening on the fatigue fracture behaviour of a partially covered surface is discussed in [20].

Discussion concerning the optimum shot peening specification is given in [21], which summarises the experimental observations. An example of the use of shot peening and a simplified theoretical approach is discussed in [22]

A unified approach to the shot peening process that can take into account the linear elastic and non-linear work-hardening material behaviour and any strain rate dependence, for a series of out-of-line or in-line impacts from arbitrary directions, has yet to be attempted. These issues can be investigated by the FEM but in this presentation we mainly focus on orthogonal normal impact for on-line and out-of-line loading-unloading and the oblique impact of a single shot.

MECHANICS OF THE SHOT PEENING PROCESS

The shot peening process is the bombardment of a deformable surface by relatively rigid spherical objects. If the energy contained in the shot exceeds the elastic resilience of the target, local plastic flow and permanent deformation will result. In addition, on rebound of the shot, the residual stresses remain locked into the target. The mechanics of the shot peening process is first examined by considering the impact of a single shot under quasi-static and dynamic loading. These analyses are then extended to multiple shots with particular impact arrangements (although limited by the number of elements we can use with current hardware limitations).

Consider a shot of radius R, density ρ impinging on a target surface with velocity v_0. At time t, if the average reaction pressure is $\bar{p}$ and the radius of the indented surface area is a, under conditions of dynamic equilibrium:

$$\frac{4\pi\rho R^3}{3}\frac{dv}{dt} + \pi a^2 \bar{p} = 0 \qquad (1)$$

The average pressure resisting the motion has been shown [14] to be given by:

$$\frac{\bar{p}}{Y} = 0.6 + \frac{2}{3}\ln\frac{EA}{YR} \tag{2}$$

where Y is the yield strength and E is the Young's Modulus of the target. (1) and (2) give:

$$\frac{\bar{z}}{R} = \left(\frac{2}{3}\right)^{\frac{1}{2}}\left(\frac{\rho v_0^2}{\bar{p}}\right)Q \tag{3}$$

where v_0 is the initial impact velocity and $\bar{z}$ is the final depth of indentation, with $\bar{p} = 3Y$ and

$$\frac{1}{Q} = \left\{\left(0.2 + \frac{2}{9}\ln\frac{E}{Y}\right) + \frac{1}{9}\left[\ln\left(\frac{2\bar{z}}{R}\right) - \frac{4\bar{z}}{R}\right]\right\}^{\frac{1}{2}}$$

As soon as the pressure reaches 3Y a rigid plastic analysis will hold. Assuming that $\bar{p}$ remains constant during the indentation process, the solution of (1) gives:

$$\frac{\bar{z}}{R} = \left(\frac{2}{3}\right)^{\frac{1}{2}}\left(\frac{\rho v_0^2}{\bar{p}}\right)^{\frac{1}{2}} \tag{4}$$

The non-dimensional number $\frac{\rho v_0^2}{\bar{p}}$ is a measure of the severity of the impact and is referred to as the "Damage Number". Under dynamic loading the material strength is influenced by the strain rate effect and this is usually taken into consideration by a power law expression, either in the form of $\frac{\sigma_d}{\sigma_{ref}} = \left(\frac{\dot{\varepsilon}_d}{\dot{\varepsilon}_{ref}}\right)^m$, where m is the strain rate index and σ_{ref} is the flow stress at a reference strain rate of $\dot{\varepsilon}_{ref}$. Alternatively, the Cowper-Symonds power law [23]:

$$\bar{\sigma}_d(\bar{\varepsilon}) = \sigma_{ref}(\bar{\varepsilon})\left[1 + \left(\frac{\dot{\bar{\varepsilon}}^{pl}}{D}\right)^{1/p}\right]$$

can be employed, where D (s^{-1}) and P are constants. If the shot rebounds from the target, provided it was initially carrying sufficient energy, a residual stress state is locked into the target surface, resulting in "shakedown". Subsequent shot impacts will not result in additional plastic flow if they generate pressures that are less than the peak pressure of the first shot.

The shot peening process is a dynamic contact problem and the associated yield criterion is position dependent. Nevertheless, the derivation outlined above and in [14] can be used to predict a residual stress state for a plate of infinite depth and for different initial impact velocities as shown in Fig. 1.

The residual stress distribution in a thin plate can be considered to be the result of additional bending and through depth "axial" stress. The resulting stress distribution is predicted to be [14]:

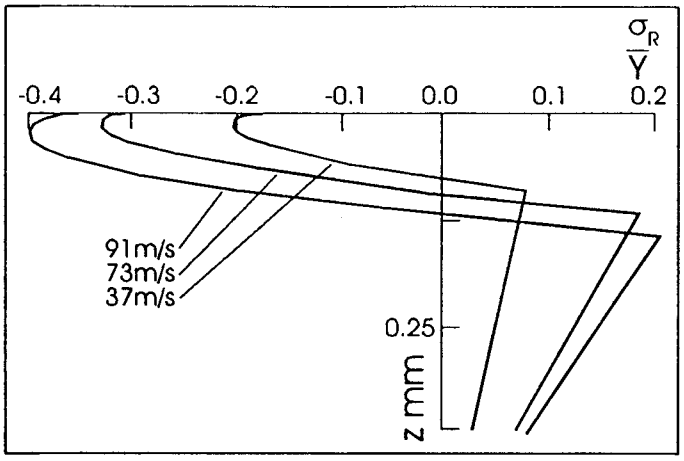

Fig. 1 –Theoretical residual stress distribution for different shot velocities [27]

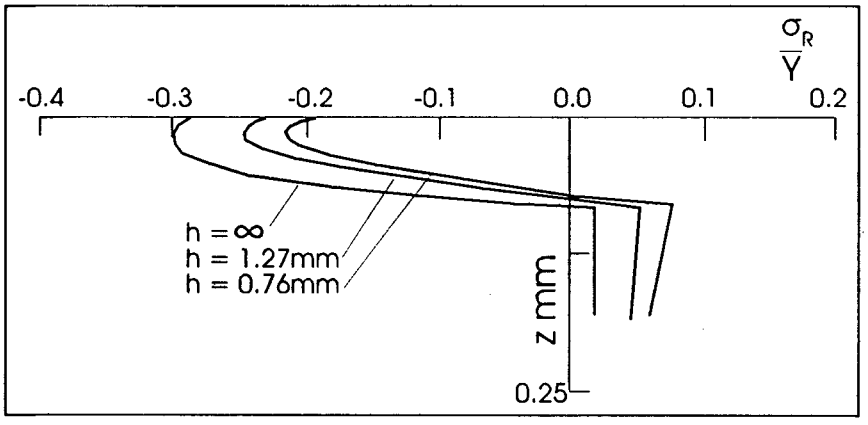

Fig. 2 - Theoretical stress distribution for different target thickness [27]

$$\sigma_R(z) = \frac{E\varepsilon_m}{1-\nu}\left\{\frac{12\lambda}{\pi h}(1-\alpha)\left(\frac{h}{2}-z\right)C_1 + \frac{2\lambda}{\pi}(1-\alpha)C_2 - \cos\pi\left[\frac{z-\alpha h_p}{2(1-\alpha)h_p}\right]1(h_p)\right\}$$

where ν is the Poisson's ratio, $1(h_p)$ is a unit step function equal to 1 for $0 \le z \le h_p$,

$$C_1 = C_2 - 2\lambda + 4\lambda\left[\frac{(1-\alpha)}{\pi}\cos\frac{\pi\alpha}{2(1-\alpha)}\right] \quad \text{and} \quad C_2 = 1 + \sin\frac{\pi\alpha}{2(1-\alpha)}$$

The predicted residual stress for an impact velocity of 37ms^{-1} for a plate thickness of h=0.76mm, 1.27mm and for a very thick target, is shown in Fig. 2. The predicted values for the various shot peening conditions shown in Figs. 1 and 2 are compared with FE simulations in section 4. Direct comparison is not actually possible because of the continual change in contact pressure between the shot and the target. Contact pressure is a function of penetration depth z and is dependent on the contact radial position $p(t,r)$ from the centre of impact. In addition, the various non-linearities of material, boundary conditions and geometry, disregarded in the theoretical approach, can be incorporated into the FE model.

DYNAMICS OF MULTIPLE SHOT PEENING

The following model arises from a detailed examination of the computed results for orthogonal in-line and out-of-line successive shot peening with deformable surfaces. When the first shot makes contact with the deformable surface, energy is transferred between the shot and the target. The shot penetrates the surface, creating a crater and producing a compressive stress field. The incompressibility of the target causes the material on the free surface to rise up around the contacting periphery of the shot. For the cases considered here, the residency prior to rebound for a rigid shot impacting on steel is approximately 1-1.5μs. It is obvious that the shot peening process is very rapid and the associated strain rate effect is very high. The plastic flow in the vicinity of the impacted zone is severe and large amounts of energy can be absorbed. The KE lost by the shot produces plastic flow through the depth of the material with a progressively diminishing strain rate.

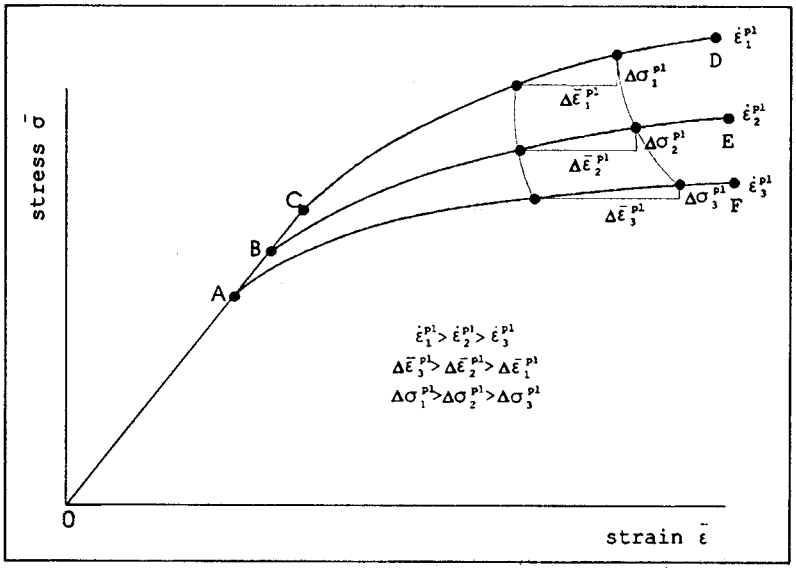

Figure 3 - Schematic presentation of incremental plastic "stress-strain" curve for a time interval of Δt, at the surface and through the material thickness

This process is shown in Fig. 3, where OABCD, OABE and OAF represent the stress-strain curves for three different strain rates of $\dot{\varepsilon}_1^{pl}, \dot{\varepsilon}_2^{pl}$ and $\dot{\varepsilon}_3^{pl}$ respectively. A plastic stress increment of $\Delta\bar{\sigma}_1^{pl}$, on OABCD, with a strain rate of $\dot{\varepsilon}_1^{pl}$ causes an increase in plastic strain of $\Delta\bar{\varepsilon}_1^{pl}$. The stress wave front propagates through the target dissipating plastic work. When it reaches a depth of Δh its strength has diminished resulting in a lower plastic stress increment in the strain rate sensitive material. Furthermore, due to the strain hardening non-linear nature of the material, the stress wave undergoes dispersion (i.e. smaller stress increments travel faster than larger ones). This will cause the stress (or associated strain) to change more gently further from the point of impact. Therefore, the stress increment deeper in the material will be something like $\Delta\bar{\sigma}_2^{pl}$ along the OABE portion of the curve associated with a strain rate of $\dot{\varepsilon}_2^{pl}$ (see Fig. 3). This stress increment produces a plastic strain increment of $\Delta\bar{\varepsilon}_2^{pl}$ which, in this case is greater than $\Delta\bar{\varepsilon}_1^{pl}$. We therefore observe a novel phenomenon associated with the shot peening process, so far not reported in the literature. The stress increment of

$\Delta\bar{\sigma}_1^{pl}(\Delta\bar{\sigma}_1^{pl} > \Delta\bar{\sigma}_2^{pl})$ on the current curve with strain rate of $\dot{\varepsilon}_1^{pl}$ is accompanied by a plastic strain increment of $\Delta\bar{\varepsilon}_1^{pl}(\Delta\bar{\varepsilon}_1^{pl} < \Delta\bar{\varepsilon}_2^{pl})$. This unexpected anomaly is the consequence of the strain rate effect of the material. Therefore, any description of this process must include the mutually inclusive effects of strain rate, plastic work dissipation and the decrease in stress wave strength and strain rate through the material thickness. The development of such a closed form solution is extremely difficult. As the wave front progresses further through the thickness of the material, the reduction in strength of the wave and the smaller amount of unspent energy, will cause a plastic stress increment of $\Delta\bar{\sigma}_3^{pl}(\Delta\bar{\sigma}_3^{pl} < \Delta\bar{\sigma}_2^{pl})$ which will be accompanied by a plastic strain increment of $\Delta\bar{\varepsilon}_3^{pl}(\Delta\bar{\varepsilon}_3^{pl} > \Delta\bar{\varepsilon}_2^{pl})$, as shown on OAF in Fig. 3.

FE SOLUTION METHODOLOGY

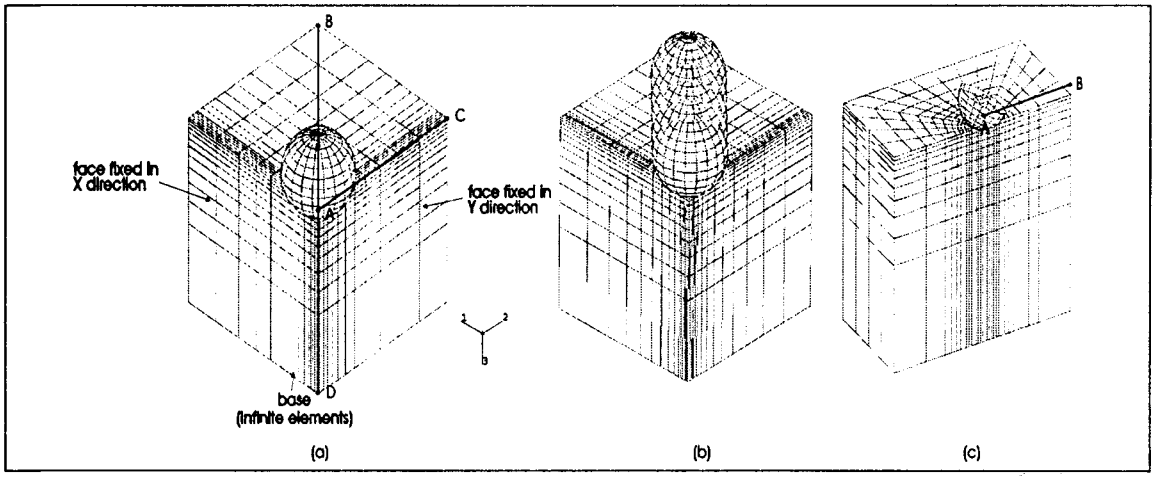

Figure 4 - Discretised models used in the shot peening simulation (a) single shot, (b) multiple shot diagonal symmetry and (c) single shot, oblique impact

Three discretised models shown in Fig. 4 were analysed using the ABAQUS FE package. The first (Fig. 4a) represents a single shot impacting onto a deformable surface under quasi static loading conditions. Separate dynamic analyses were also performed for the three velocities shown in Figs. 1 and 2. Fig. 4b shows five spheres projected normally onto the target surface in a diagonal line. Fig 4c is a single shot fired at the target at an oblique angle. In each case the shot was modelled by a spherical rigid surface with a mass was positioned at its centre. The in-line configuration (Fig. 4b) was arranged so that successive shots did not collide before or after rebound.

MODEL SHAPE AND DIMENSIONS

Target

A solid steel block of width, breadth and height 4, 4 and 2 mm, respectively was used in the analyses. The loading modes were selected so that the model exhibits a double symmetry, hence only ¼ of it needs to be modelled. 3-D 8 noded brick elements were used with a mesh density of 14 elements in each direction. The mesh was graded in all three directions so that the smallest elements occurred in the vicinity of the impact. The total number of elements used in

each of the models shown in Fig. 4 were:

Element type	No. used
3-D 8 noded brick, C3D8I	2156
3-D 8 noded infinite elements, CIN3D8	196
Point Mass elements	1/ 5

Rigid Surfaces and Mass Elements

Spherical rigid surfaces of diameter 0.72 mm, were used to model the shot. Each rigid surface carried a mass element appropriate to model the full mass of the shot (1.5128 mg). In the second case (Fig. 4b) the spheres were arranged above one another with a vertical separation of 0.085mm and a horizontal separation of 0.1 mm along the diagonal. This meant that the impacts overlapped in successive collisions. The vertical separation of the spheres meant that, for an initial collision velocity of 66.67 ms^{-1}, the time lag between consecutive impacts was 1.27 μs which was greater than the contact residency time. The rigid surfaces were modelled so that no interference between the incoming and rebounding shots occurred.

Boundary Conditions

As shown in Fig. 4, the imposition of double symmetry requires that the vertical planes were fixed in the x and y directions. Originally the base of the model was fixed in the axial z direction. However, this created a boundary which reflected the stress waves propagating from the impact zone and so the model was redefined with a layer of infinite elements. Any material subjected to shot peening will have supported anchorages but comparison of results from models using infinite elements and finite elements fixed in the z direction showed that there was little difference in the stress levels obtained. In the first two impact cases (Figs. 4a and 4b), the rigid surfaces were fixed in all degrees of freedom except for translation in the z direction. In the second case considered (Fig. 4b) the shot impacts lie along the diagonal and successive shots impact in the indentation left by a previous impact. Therefore, although the first shot would rebound vertically, the second and subsequent shots would rebound at an oblique angle with a small horizontal component of velocity. However this component was suppressed in this analysis. Extra analyses were performed using a model incorporating additional translational degrees of freedom for the shot in the horizontal plane. It was found that the vertical rebound velocities were approximately the same as when these degrees of freedom were removed and that the horizontal components of velocity were an order of magnitude less than the vertical component. This investigation therefore concentrates on the vertical components of shot velocity and displacement.

Contact and Constraint Conditions

Contact between shot and target was established by using a "master-slave" contact pair [24] and the ABAQUS default of isotropic Coulomb friction was used, which assumes the critical surface tractions to be proportional to the contact pressure and the coefficient of friction (taken as 0.1).

In the case represented by Fig. 4b, the upper surface of the target was designated by 5 slave surfaces, each one targeted against a master surface associated with by the relevant rigid shot.

MATERIAL PROPERTY

The target was assumed to be made of high tensile steel, with a linear elastic stress-strain relationship which had a modulus of elasticity $E = 2.03 \times 10^5$ Nmm^{-2}, a Poissons ratio of $\nu = 0.3$ and a mass density $\rho = 7830$ kgm^{-3}. The material work hardening under static loading conditions

was assumed to be bi-linear, and the relationship between plastic strain and the accompanying yield stress is given in Table 1.

Table 1: Material Non-linear Work Hardening

Stress σ Nmm^{-2}	1250	1550
Plastic strain ε^p	0.0	1.0

The material was assumed to exhibit a strain rate dependence under dynamic loading. This was expressed by a relation similar to that proposed by Cowper-Symonds' power law [23]:

$$\sigma = \sigma(\varepsilon)\left[1+\left(\frac{\dot{\varepsilon}^{pl}}{D}\right)^{1/p}\right]$$

where $\sigma(\varepsilon)$ is the static stress-strain relation, $\dot{\varepsilon}^{pl}$ is the plastic strain rate and D and P are adjustable parameters, influencing the material's constitutive response behaviour. Calculations of the equivalent plastic strain rate from the analyses showed values in the region of 0.5 μs^{-1}. The strain rate was highest for the case of multiple shot impacts, where the ridges formed by previous impacts provided different initial contact conditions (a smaller contact area) than in the case of impacts at the same point. Yu and Jones [25] used values of D = 1.05 x 10^7 s^{-1} and P = 8.30 for large strains up to rupture in their studies of the failure of clamped beams. However, they and others suggest that yield stress and flow stress is much more strain-rate sensitive at small strains. Taking this into consideration, the values of D = $40s^{-1}$ and P = 5.1 were chosen so that the effects of strain rate at its peak value would not enhance the material behaviour by more than 50-70%.

RESULTS AND DISCUSSION

Single Shot Simulation

Fig. 5 shows the results of the single shot simulation. The variation of residual stress with depth for three impact velocities (37, 73 and 91 ms^{-1}) and for a static analysis is shown in Fig. 5a. The results from the dynamic simulation can be compared with the theoretical results shown in Fig. 1 [14]. A direct comparison maybe somewhat misleading because of the effects of nonlinear workhardening, strain rate dependence and the rebound of the shot from the target surface which are included in the Finite Element solution but not in the theoretical treatment. The phase diagrams for the three velocity cases are given in Fig. 5b. The greater the impact velocity, the higher the rebound velocity.

Muliple In-line Shot Simulation

The displacement-time and velocity-time histories for the diagonal line of 5 shots (Fig 4b) are presented in Fig. 6. The contact time is approximately 0.6μs, and the rebound velocity of successive shots gets progressively smaller. This is due to the plastic field generated by the first shot impact, which is enhanced by the impact of the other shots, depositing more energy in the form of plastic work dissipation in the peened material. Fig. 7 shows the variation of residual axial stress with depth along a line under the impact point of each shot parallel to AD of Fig. 4a at times of maximum indentation. The axial (S_{33}) stresses at the surface of the material are zero and a state of internal self equilibrium has been attained.

Fig. 8 shows the variation of axial stress computed at the node nearest the impact of each shot. The variation shown for shot 5 is probably due to the fact that the nearest node was some distance from the point of impact between slave and master surfaces (target and shot).

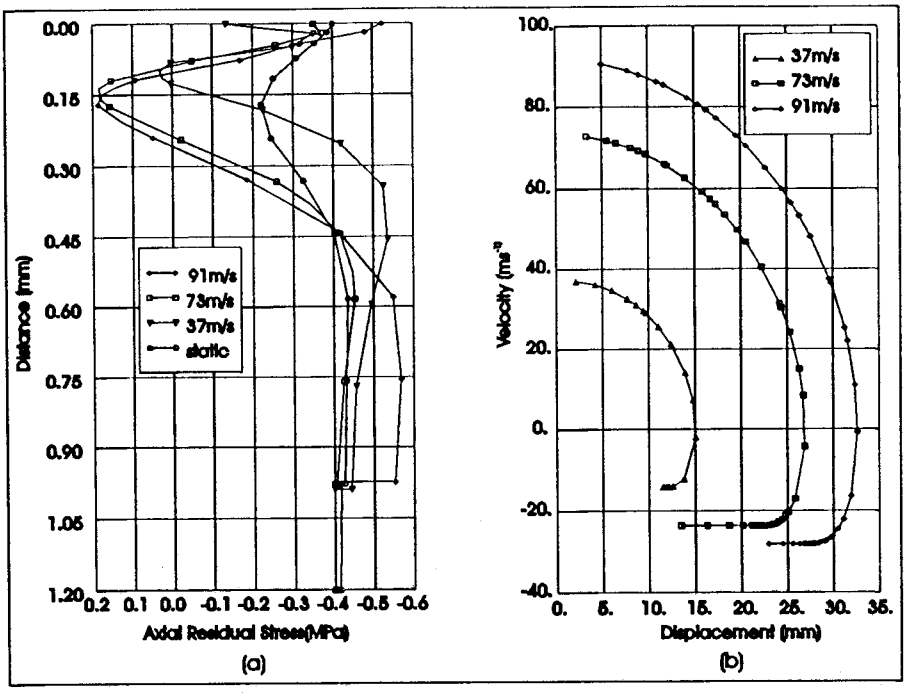

Figure 5 - (a) Variation of residual stress with depth for three dynamic and one static FE analyses of single shot impact (b) Phase diagrams for three dynamic single shot analyses

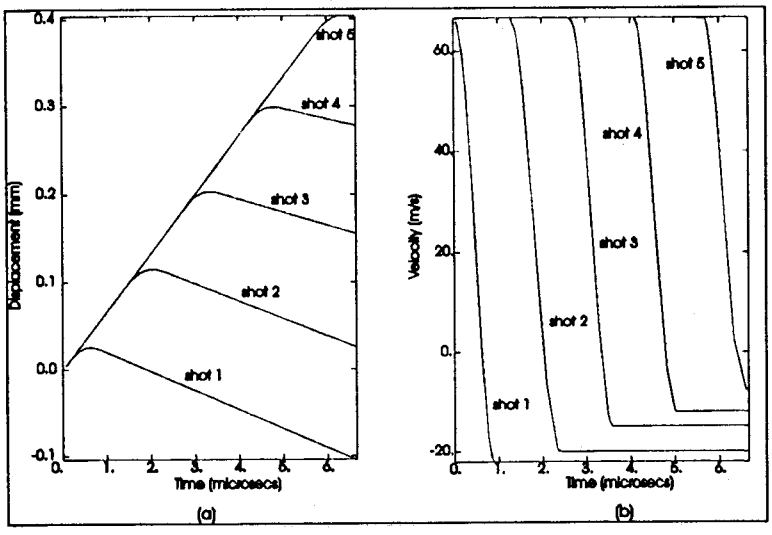

Figure 6 - (a) displacement and (b) velocity - time plots for FE simulation, 5 shot normal impact

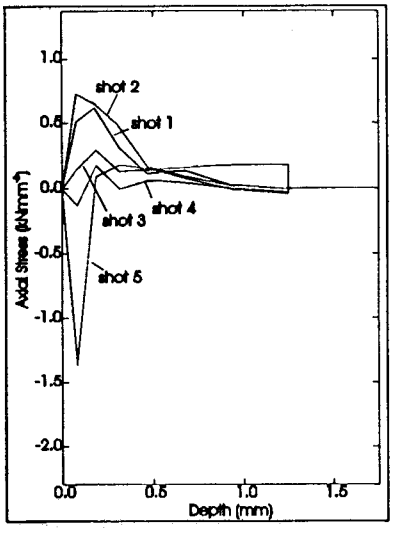

Figure 7 - Axial stress variation with depth at max displacement

Fig. 9 shows how the axial stress varies with depth (positions 1 to 5 refer to the nodes along the line AD of Fig. 4a starting from the point directly under the impact of the first shot). It was this variation in stress with depth that led to the proposition that the stress-strain dependence relies on strain-rate as described by Fig. 3. Overlapping shot impacts have a marked effect on the stress time history due to the rise in the periphery of the contact area. Fig. 10 shows the variation in equivalent plastic strain at alternate nodal points along the line AC in Fig. 4a.

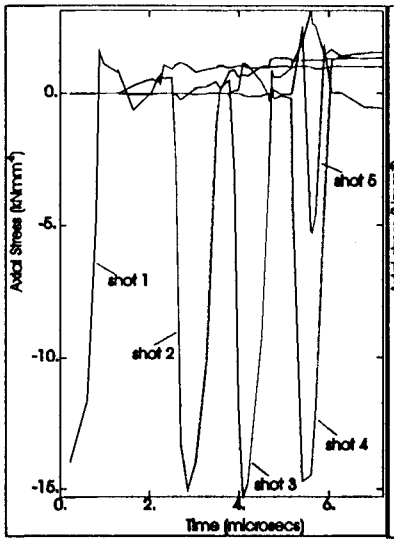

Figure 8 – Axial stress at node closest to impact of each of 5 shots

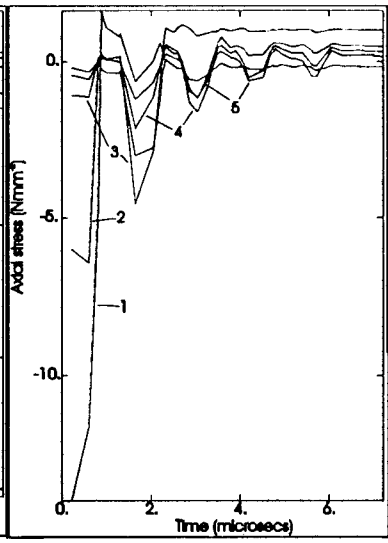

Figure 9 – Variation in axial stress with time along line AD of Fig. 4a

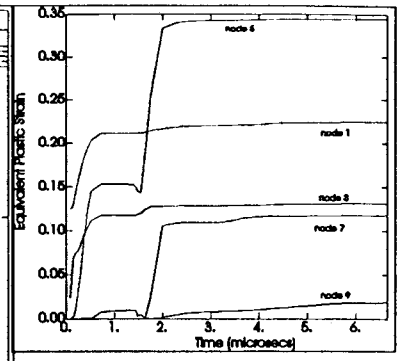

Figure 10 – Plastic equivalent strain at alternate nodal points along the line AC in Fig. 4a for the single shot oblique impact simlation

Single Shot, Oblique angle impact simulation

The model for the single shot oblique impact simulation is shown in Fig. 4c. The variation in axial (S_{33}) stress with depth in the material (vertically below the point of impact) is shown in Fig. 11 at .03, .08, .17, .35, .44, .52 microseconds after impact. Fig. 12 shows how the axial stress varies at the surface of the target (along the line AB in Fig. 4c) for the same times after impact.

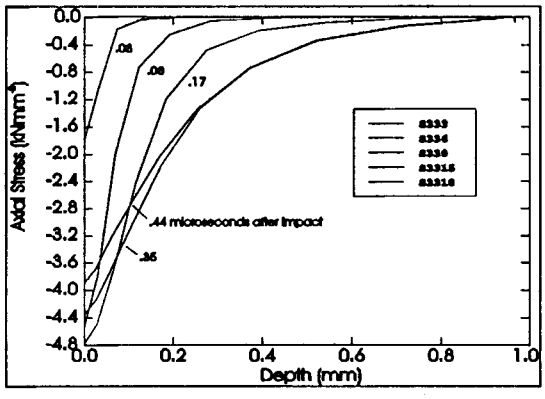

Figure 11 - Axial stress as a function of depth at point of impact for times indicated for the single shot oblique impact simulation

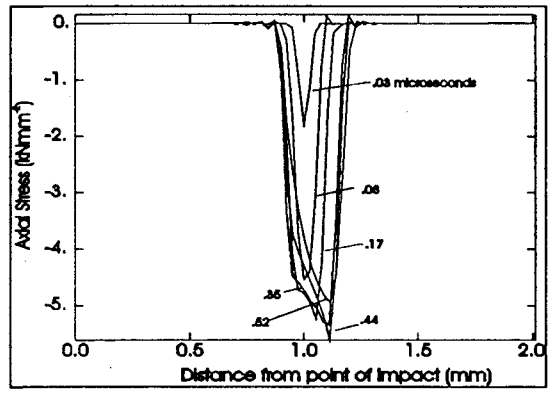

Figure 12 - Axial stress along the surface of the target (line AB in Fig. 4c) from the point of impact at times indicated for the single shot oblique impact simulation

CONCLUSIONS

The shot peening of a target, with non-linear work hardening and strain rate dependency, is a complex process. The model discussed above describes the important role that strain rate plays in the distribution of stresses. It can be applied to multiple shot peening without the need to make any simplifying assumptions about material behaviour or geometrical and boundary non-linearities. By using a strain-hardening strain-rate sensitive material it is possible to model the

effects that the repeated and progressive impacts of shots have on the stress profile and extent of surface hardening. The technique provides a useful and versatile tool for further investigation. However, the results presented should be viewed with caution until experimental supporting evidence becomes available.

REFERENCES

1. Hertz, H. "Uber die Beruhrong fester elastischer Korper J. Fur reine und angewandte Mathematik "(Creffe) Vol 92, p.155, 1881
2. Boussinesq, J. "Application des Potentials" Comptes Rendus, 114, p1150, 1892
3. Timoshenko, S. and Goodier, J.N. "Theory of Elasticity", 2nd edition, McGraw Hill New York, 1951
4. Sneddon, J.N. "Fourier Transforms", McGraw Hill, New York, 1951
5. Goldsmith, W., "Impact". Arnold, London, 1960
6. Johnson, W. "Impact Strength of Materials", Arnold, London, 1972
7. Ishibishi, T, and Shimoda, S., "The influences of mechanical properties of spherical indentors on hardness", Bulletin of JMSM, Vol 29, No 258, Dec 1986, pp 4013-4019
8. Ishibishi, T, and Shimoda, S., "The correlation between hardness and flow stress", JSME International Journal, Series 1, Vol 31, No 1, pp 117-125, 1988
9. Al-Obaid, Y.F., "Three dimensional dynamic finite element analysis for shot peening mechanics", Computers and Structures, Vol 36, No 9, pp 681-689, 1990
10. Al-Obaid, Y.F., "A rudimentary analysis of improving fatigue life of metals by shot peening", Transcript of the ASME, Journal Applied Mechanics, Vol 57, pp 307-312, June 1990
11. Al-Obaid, Y.F., "The automated simulation of dynamic non-linearity to shot peening mechanics", International Journal of Computing Structure, Vol 90, No 6, pp 1451-1460, 1991
12. Al-Hassani, S.T.S., "Mechanical aspect of residual stress development in shot peening", 1st International Conference on Shot Peening, Sept 1981, Paris
13. Al-Hassani, S.T.S., "Shot peening of metals, mechanics and structures", SAE paper, 821452, 1982
14. Al-Hassani, S.T.S., "An Engineering Approach to Shot Peening Mechanics", Proceedings ICSP-II Chicago, Illinois, The American Shot Peening Society, Paramus, NJ, 1984, pp 275-282.
15. Meguid, S.A., and Iclair, M.S., Proceedings ICSP-II Chicago, Illinois, The American Shot Peening Society, Paramus, NJ, p 306, 1984
16. Li, J.K., Mei Yao and Duo Wang, "Mechanical approach to the residual stress field induced by shot peening", Material Science and Engineering, A147, 1991, pp 169-173
17. Hills, D.A., Waterhouse, R.B., and Noble, B., "An analysis of shot peening", Journal of Strain Analysis, Vol 18, No 2, IMechE, 1983
18. Khabou, M.T., Castex, L., and Inglebert, G., "The effect of material behaviour on the theoretical shot peening results", European Journal of Mechanics, A/Solids, Vol 9, No 6, 1990, pp 537-549
19. Tirupataiah, Y., and Sundararajan, G., "A dynamic indentation technique for the characterization of the high strain plastic flow behaviour of ductile metals and alloy", Journal Mechanics Phys Solids, Vol 39, No 2, pp 243-271, 1991
20. Meguid, S.A., "Effect of partial coverage upon the fatigue behaviour of peened components", Fatigue Tact. Engineering Materials Structure Vol 14, No 5, pp 515-530, 1991
21. Lawreng, M., and Ekis, I., "Optimum shot peening specification I", Geor Tech, Vol 8, No 6, pp 15-22, 1991
22. Homer, S.E., and VanLuchene, R.D., "Aircraft wing skin contouring by shot peening", Journal Material Shaping Technology, Vol 9, No 2, pp 89-101, 1991
23. Symonds, P.S., "Viscoplastic behaviour in response of structures to dynamic loading", Ed N.J. Muffington, ASME, New York, pp 106-125, 1965
24. Hibbitt, Karlson & Sorenson, Inc., "Abaqus User's manual ver 5.7", HKS, Pawtucket, RI, 1997.
25. Yu, J. And Jones, N., "Further Experimental Investigations on the failure of clamped beams under impact loads", Int. J. Solids Structures, Vol. 27, No. 9, pp 1113-1137, 1991.